Demography
https://doi.org/10.1007/s13524-019-00842-x

Population Pyramids Yield Accurate Estimates of Total Fertility Rates

Mathew E. Hauer[1] · Carl P. Schmertmann[2]

Published online: 28 January 2020

Abstract

The primary fertility index for a population, the total fertility rate (TFR), cannot be calculated for many areas and periods because it requires disaggregation of births by mother's age. Here we discuss a flexible framework for estimating TFR using inputs as minimal as a population pyramid. We develop five variants, each with increasing complexity and data requirements. We test accuracy across a diverse set of data sources that comprise more than 2,400 fertility schedules with known TFR values, including the Human Fertility Database, Demographic and Health Surveys, U.S. counties, and nonhuman species. We show that even the simplest and least accurate variant has a median error of only 0.09 births per woman over 2,400 fertility schedules, suggesting accurate TFR estimation over a wide range of demographic conditions. We anticipate that this framework will extend fertility analysis to new subpopulations, periods, geographies, and even species. To demonstrate the framework's utility in new applications, we produce subnational estimates of African fertility levels, reconstruct historical European TFRs for periods up to 150 years before the collection of detailed birth records, and estimate TFR for the United States conditional on race and household income.

Keywords Indirect estimation · Total fertility · Bayesian models

Introduction

Fertility is the primary engine of global population change (Gerland et al. 2014) and is central to the United Nations' Sustainable Development Goals for female education,

Electronic supplementary material The online version of this article (https://doi.org/10.1007/s13524-019-00842-x) contains supplementary material, which is available to authorized users.

✉ Mathew E. Hauer
mehauer@fsu.edu

[1] Department of Sociology and Center for Demography and Population Health, Florida State University, Tallahassee, FL 32306, USA

[2] Department of Economics and Center for Demography and Population Health, Florida State University, Tallahassee, FL 32306, USA

child and maternal mortality, gender equality, and reproductive health (Abel et al. 2016). The total fertility rate (TFR) is a critical component of population change, and scientists and practitioners use it in a wide range of applications.

The conventional technique for calculating TFR is straightforward but requires data on births disaggregated by age of mother. This makes TFR incalculable for (1) countries and regions that lack detailed birth records or quality survey data; (2) historical populations that predate vital event registration; (3) small-area populations for which reporting agencies mask birth records for privacy reasons; and (4) any subpopulation not identified on official birth records, such as women in a specific income decile, religion, tribe, or occupation. The need for disaggregation of births by mother's age thus limits fertility analysis mainly to large populations in contemporary countries with good vital registration systems or country-periods with quality survey data on fertility.

Demographers have proposed various indirect estimation techniques to circumvent these limitations (Bogue and Palmore 1964; Rele 1967). However, these methods often rely on variables (e.g., mean age at marriage, percentage of women ever married) that may be absent from census or survey data. Thus, existing indirect methods—much like direct calculation of TFR—are typically limited to areas, periods, and populations with sufficiently detailed data. In addition, relationships between fertility and social indices can differ over time and over populations, making indirect methods error-prone when applied outside the context from which regression coefficients were derived (Hauer et al. 2013; Tuchfeld et al. 1974).

Here we discuss a flexible framework for estimating TFR. We derive a suite of five TFR estimators that overcome the aforementioned limitations. Two of these estimators are based on previous work (Hauer et al. 2013; Schmertmann and Hauer 2019); three derivations are new. Our framework uses census or survey counts of population by age and sex as inputs, and it exploits demographic relationships between TFR and population pyramids. Its principles are straightforward and well known. In previous research, we demonstrated that errors for this method tend to be smaller than those for other indirect methods (Hauer et al. 2013) and that minor modifications using commonly available data lead to further improvements (Schmertmann and Hauer 2019). In this article, we present several new variants and offer a robust evaluation of the framework across a wide range of demographic situations.

We describe the framework's derivation and evaluate the accuracy of several variants over a wide variety of databases. We test the accuracy using known TFRs for 2,403 fertility schedules, spanning 124 years, across various scales, mortality regimes, and fertility levels. We also offer examples of TFR estimation for new types of data.

Methods and Materials

Demographic Relationships Between TFR and Age-Sex Distributions

Using $f(a)$ to denote the density of fertility at exact age a, the period total fertility rate is $TFR = \int_{\alpha}^{\beta} f(a)\, da$, which is usually approximated as

$$TFR = n \cdot \sum_{a=\alpha}^{\beta-n} F_a = n \cdot \sum_{a=\alpha}^{\beta-n} \frac{B_a}{W_a}, \tag{1}$$

where $[\alpha, \beta)$ is the reproductive age range, W_a is the midyear population of women in the n-year age interval $[a, a+n)$ (hereafter called *age group a*), B_a is the annual number of births to those women, and F_a is their average fertility rate. Demographers commonly use $(\alpha, \beta, n) = (15, 50, 5)$, in which case there are seven age groups with fertility rates $F_{15}, F_{20}, \ldots, F_{45}$, and $TFR = 5 \cdot \sum F_a$.

Data for population pyramids are also reported for age groups, usually with $n = 5$. Analysis of relationships between TFR and the relative numbers of women and children by age group requires consideration of several demographic factors. First, not all children born during the previous n years will still be alive at the time a population is enumerated. Second, not all women who gave birth over the past n years will still be alive to be counted. Third, surviving women in a given n-year age group at the time of enumeration were in that age group for only a fraction of the past n years.

These are all familiar considerations for demographers. As we demonstrated elsewhere (Schmertmann and Hauer 2019), a slight rearrangement of standard Leslie matrix formulas (e.g., Wachter 2014) for age groups of width $n = 5$ shows that the expected number of surviving children under age 5 per surviving woman in age group a at the end of a five-year period is

$$C_a = \left[\frac{L_{a-5}}{L_a} \cdot F_{a-5} + F_a\right]\frac{L_0}{2} = TFR \cdot \frac{L_0}{5} \cdot \frac{1}{2}\left(\frac{L_{a-5}}{L_a} \cdot \phi_{a-5} + \phi_a\right) = TFR \cdot s \cdot p_a, \quad (2)$$

where $\phi_a = 5F_a/TFR$ is the fraction of lifetime fertility occurring in age group a for a synthetic cohort subject to current period rates; L_a is expected person-years lived in age group a in a life table with a radix $l_0 = 1$; $s = L_0/5$ is the expected fraction still alive among children born in the past five years; W_a is the observed women in age group a; and W is the total number of women enumerated at childbearing ages [15, 50).[1]

C_a is the product of three multiplicative factors: TFR, child survival s, and an age-specific term p_a that represents the proportion of lifetime fertility experienced over the past five years by females in age group a. The expected total number of surviving 0- to 4-year-olds is therefore

$$C = \sum_{a=15}^{45} W_a C_a = W \cdot p \cdot s \cdot TFR, \quad (3)$$

where $p = \sum W_a p_a / W$ is the population-weighted mean of p_a values. A more intuitive version of Eq. (3) in terms of units is

$$\underbrace{Children\ 0-4}_{C} = \underbrace{women}_{W} \cdot \underbrace{\frac{births\ in\ last\ 5\ yrs}{lifetime\ births}}_{p} \cdot \underbrace{\frac{surviving\ children\ 0\text{–}4}{births\ in\ last\ 5\ yrs}}_{s} \cdot \underbrace{\frac{lifetime\ births}{woman}}_{TFR}.$$

We then rearrange Eq. (3) as an expression for TFR:

$$TFR = \frac{1}{s} \cdot \frac{1}{p} \cdot \frac{C}{W}. \quad (4)$$

The most fundamental assumption behind any estimators of period TFR derived from Eq. (4) is that the number of young children observed in an age pyramid can, after

[1] We assume that fertility is 0 outside this range, so $F_{10} = 0$ in Eq. (2) when $a = 15$.

suitable correction for child mortality, serve as a proxy for recent births to the women who are counted in that same age pyramid. The age pyramid in question could come from a national census or from a regional disaggregation of national populations, but it could also come from a survey in which one can identify households in a chosen category—for example, by education of householder, geographic location, or total income. In the latter cases, we count the young children and the reproductive-age women within households that belong to the chosen category.

As long as women and their own children are counted in the same age pyramid, changes caused by internal migration (or more generally, caused by any kind of change of category) are not a major concern. The relationships in Eq. (4) still hold for open populations. Changes of category or location can affect the *interpretation* of TFR, however. Our measures use fertility over a five-year period, and cross-sectional input data come from the *end* of that period. If changes of status are related to fertility, then indices that condition on end-of-period status may not always capture the rates that we would most like to have. For example, if single women are likely to marry quickly after having children, then an estimator based on cross-sectional data of unmarried women would accurately estimate "period fertility of women who end up unmarried" but not "period fertility of women while unmarried." Similar issues of interpretation would arise if central city residents tended to move to suburbs a short time after becoming parents. These difficulties are conceptual rather than empirical, but for stratified subpopulations, it is important to understand how conditioning on end-of-period status affects interpretation of TFR: indices derived from Eq. (4) describe the *recent* fertility of those in the chosen category *at the time of the cross-sectional census or survey.*

In the following sections, we derive five methods for estimating period TFR from the demographic relationship in Eq. (4), each with different data inputs. Table 1 shows the input data for each variant (*iTFR*, *xTFR*, *iTFR*+, *xTFR*+, and *bTFR*). It is possible to use the *iTFR* and *xTFR* variants with age pyramid data only. If q_5 estimates are also available, then it is possible to use *iTFR*+, *xTFR*+, and *bTFR*.

Implied Total Fertility Rate: *iTFR*

The simplest approximation to Eq. (4) assumes that child mortality is close to 0 ($s \approx 1$) over the first n years of life and that women are uniformly distributed over 35 years of reproductive ages ($p \approx n/(\beta - \alpha) = 5/35 = 1/7$). Following (Hauer et al. 2013), we call the resulting estimator the *implied total fertility rate* (*iTFR*):

$$iTFR = \frac{\beta - \alpha}{n} \cdot \frac{C}{W} = 7 \cdot \frac{C}{W}.$$

For human populations divided into five-year age groups ($(\alpha, \beta, n) = (15, 50, 5)$), $iTFR = 7 \cdot C/W$. For other species or other age combinations, the C/W multiplier may differ based on differences in (α, β, n).

Extended Total Fertility Rate: *xTFR*

Our second estimator uses details from the population pyramid to improve the approximation of the $1/p$ term in Eq. (4). The *iTFR* formula uses $1/p = 7$, which is correct if

Table 1 Characteristics of alternative TFR estimators

	Adjust for Child Mortality?	
Use Age Distribution Detail for Women 15–49?	No	Yes
No	*iTFR*	*iTFR*⁺
Yes	*xTFR*	*xTFR*⁺, *bTFR*

Notes: bTFR is a probabilistic, Bayesian version using statistical distributions for unknown demographic quantities. Other estimators are deterministic.

women enumerated in the age-sex pyramid experienced a (mortality-adjusted) average of one-seventh of lifetime fertility over the previous five years. In practice, this is not exactly true because reproductive-age women may be concentrated in high- or low-fertility age groups. For example, if the age pyramid has a high concentration of women in their late 20s and early 30s, then typical age patterns of human fertility make it likely that they have just passed through five especially high-fertility ages, that $p > 1/7$, and that the multiplier $1/p < 7$. Conversely, a high concentration of women aged 40–49 in the age pyramid implies a multiplier $1/p > 7$.

Although $1/p = 7$, as in *iTFR*, often leads to small errors, it is possible to improve the estimator by using additional details from the population pyramid. In previous research (Schmertmann and Hauer 2019), we noted that the necessary adjustments can be large for small populations such as U.S. counties that have substantial variations in the age distributions of reproductive-age women.

To learn about the $1/p$ multipliers, we examined 1,804 fertility schedules in the Human Fertility Database (HFD n.d.) for which the true TFR is known. For each country c and time t, we calculate the average TFR over the five previous years, $TFR^*_{ct} = 1/5\sum_{k=0}^{4} TFR_{c,t-k}$, and the empirical values of TFR^*_{ct} divided by observed child-woman ratios C_{ct}/W_{ct}. In other words, we calculated the multipliers necessary to convert $C/W \rightarrow TFR^*$ under the assumption of negligible child mortality. The *iTFR* formula assumes that this multiplier equals 7. In the HFD, these multipliers are within 10% of 7 (6.3–7.7) in 88.6% of country-years.

As in previous empirical examples (Schmertmann and Hauer 2019), there is a notable correlation between the age distribution of women and the multiplier. Using the proportion of women aged 25–34 among those who are aged 15–49 (π_{25-34}) as a predictor in a simple regression with HFD data produces the approximation $TFR^*_{ct}/(C_{ct}/W_{ct}) \approx 10.65 - 12.55\ \pi_{25-34}$, which we use to define the *extended TFR*, or *xTFR*, estimator:

$$xTFR = (10.65 - 12.55\ \pi_{25-34}) \cdot \frac{C}{W}. \tag{5}$$

xTFR adjusts for non-uniform distributions of women within reproductive ages.[2] For any given child-woman ratio, *xTFR* produces a lower estimate for lifetime fertility when women are more concentrated in high-fertility age groups.

[2] The coefficient values 10.65 and –12.55 are appropriate when W includes women aged [15, 50). Researchers could use a similar regression procedure with HMD data to produce different coefficients for other definitions of the reproductive age span.

Measures Adjusting for Child Mortality: *iTFR*⁺ *and xTFR*⁺

Because our derivations for *iTFR* and *xTFR* assume no child mortality, the survival multiplier in Eq. (4) is ($1/s \approx 1$). These simple formulations are parsimonious and generally accurate for populations with low to moderate mortality. However, when mortality levels are higher, it is logical that TFR would be underestimated and that errors would increase.

Our third and fourth estimators, denoted *iTFR*⁺ and *xTFR*⁺, approximate the $1/s$ component in Eq. (4) using estimated under-5 mortality. Specifically, we use $1/s \approx 1/(1 - 0.75\, q_5)$, which is based on both logical and empirical relationships between life table variables. In 266 years of Swedish HMD data, with under-5 survival rates ranging from 0.661 (in 1773) to 0.998 (in 2014), the approximation $\hat{s} = 1 - 0.75\, q_5$ had a correlation with s of .999. Over these 266 years, replacing true multipliers $1/s$ with approximations $1/s$ in Eq. (4) would produce very slight underestimates of TFR, ranging from –3.3% to –0.03%, with a median underestimate of –0.93%.

We call the variants that include simple adjustments for child mortality *iTFR*⁺ and *xTFR*⁺. Specifically,

$$iTFR^{+} = \left(\frac{7}{1 - 0.75\, q_5}\right) \cdot \frac{C}{W} \tag{6}$$

$$xTFR^{+} = \left(\frac{10.65 - 12.55\, \pi_{25-34}}{1 - 0.75\, q_5}\right) \cdot \frac{C}{W}. \tag{7}$$

A Probabilistic Model: *bTFR*

Our fifth estimator, *bTFR*, is a fully probabilistic Bayesian model. It uses details from the population pyramid about female age structure within reproductive ages, and it requires an estimate of under-5 mortality.

The Bayesian approach treats the number of children as a Poisson random variable and treats the demographic quantities in Eqs. (2) and (3) as uncertain. We derive prior distributions for the fertility and mortality patterns that determine p and s from large demographic databases (Human Fertility Database (HFD) n.d.; HMD n.d.). We define the *bTFR* estimator as the median of the marginal posterior distribution of a population's TFR, conditional on observed C and (W_{15}, …, W_{45}). Because they are probabilistic, *bTFR* estimators automatically produce uncertainty measures as well as point estimates. We describe this method in detail elsewhere (Schmertmann and Hauer 2019). We briefly summarize here.

Fertility Parameters

The proportion of lifetime fertility experienced by women in the five years before a census or survey depends on their age distribution (which is observed) and on the relative levels of fertility in different age groups (which are uncertain). To model this uncertainty, we decompose the fertility schedule for five-year age groups into level and shape

components, $(F_{15}, ..., F_{45}) = \frac{TFR}{5} \cdot (\phi_{15}, ..., \phi_{45})$. As in our prior work (Schmertmann and Hauer 2019), we model the proportions $\phi_{15}, \ldots, \phi_{45}$ in terms of log odds, $\gamma_a = \ln(\phi_a / \phi_{15})$ for $a = 15, \ldots, 45$, and then translate as $\phi_a(\gamma) = \exp(\gamma_a) / \sum_z \exp(\gamma_z)$. By construction, these seven ϕ_a values are positive and sum to 1.

Our model for the γ indices is $\gamma = m + \mathbf{X}\beta$ where $m = (0\ 1.39\ 1.59\ 1.23\ 0.45\ -0.89\ -3.44)'$ and $\mathbf{X} = \begin{pmatrix} 0 & 0.27 & 0.54 & 0.73 & 0.88 & 1.04 & 1.52 \\ 0 & 0.32 & 0.51 & 0.51 & 0.35 & 0.05 & -0.72 \end{pmatrix}'$ are constants derived from empirical data, and β are unknown shape parameters (for details, see Schmertmann and Hauer 2019).[3] When combined with a prior distribution $\beta \sim N(0, I_2)$, this model assigns higher prior probabilities to fertility age patterns that are more similar to those in the HFD and the U.S. Census Bureau's International Database (United States Census Bureau 2016).

We use an uninformative prior for *TFR*: $TFR \sim \text{Uniform}(0, 20)$. This allows the level of total fertility to be determined almost completely by the data, rather than by prior assumptions.

Mortality Parameters

We model child and adult mortality with a relational mortality model (Wilmoth et al. 2012), in which two parameters describe the complete pattern of mortality rates by age: the probability of death before age 5 (q_5) and a shape parameter k with typical values between –2 and +2. The model uses fixed constants $\{a_x, b_x, c_x, v_x\}$ derived from mortality schedules in the HMD:

$$\ln\mu_x(q_5, k) = a_x + b_x[\ln q_5] + c_x[\ln q_5]^2 + v_x k, x = 0, 1, 5, 10, ..., 45. \quad (8)$$

We use standard demographic calculations to convert these log mortality rates into the L_a values in Eq. (2).

To account for possible errors in estimated mortality, we use a beta distribution for the true value of q_5. Our prior is $q_5 \sim \text{Beta}(a, b)$ with a and b such that $P[q_5 < 1/2\min(\hat{q}_5)] = P[q_5 > 2\max(\hat{q}_5)] = .05$. This prior allows for a considerable amount of possible error in the q_5 estimate used as input: it assigns a 90% prior probability that the true value of q_5 is between one-half and twice its estimated value. For the shape parameter k, our prior is $k \sim N(0, 1)$. We assume *a priori* that mortality parameters q_5 and k are independent.

Complete bTFR Model

Any set of parameters (*TFR*, β, q_5, k) implies specific values of C_a in Eq. (2). The expected number of surviving children to the W_a women observed in age group a is

[3] The highest values in m correspond to age groups [20, 25) and [25, 30), so that those age groups represent the highest shares of lifetime fertility. Because the first column of $\mathbf{X}$ has monotonically increasing values, the first element of β affects the mean age of childbearing: higher values raise the log odds of late relative to early fertility. Similarly, the second element of β affects the variance of age-specific fertility, with higher β_2 causing higher concentration of fertility in the 20s and lower variance.

W_aC_a, and the observed number of surviving children to these women is a Poisson random variable with mean W_aC_a.[4] Assuming statistical independence across maternal age groups, the total number of children also has a Poisson distribution:

$$C|W, TFR, \beta, q_5, k \sim Poisson\left[\sum_{a=15}^{45} W_a C_a(TFR, \beta, q_5, k)\right]. \quad (9)$$

The posterior distribution of parameters conditional on age pyramid data is therefore

$$P(TFR, \beta, q_5, k|C, W) \propto L(C|W, TFR, \beta, q_5, k) f_\beta(\beta) f_q(q_5) f_k(k), \quad (10)$$

where the likelihood (L) is Poisson, and the f functions represent the prior densities for unknown parameters. The flat prior for *TFR* does not affect the posterior distribution over the range $TFR \in [0, 20]$.

The marginal posterior for *TFR* provides the relative probabilities of alternative fertility levels, given the number of children (C) and the counts of women (W_{15}, …, W_{45}) in the observed age pyramid. We sample from the joint posterior distribution Eq. (10) using Markov Chain Monte Carlo (MCMC) methods, programmed in *Stan* (Carpenter et al. 2017) using the *rstan* package in *R* (R Core Team 2016; Stan Development Team 2016), and we estimate the marginal posterior of *TFR* using the empirical density of sampled *TFR* values.

Data

To evaluate the accuracy of the five estimators over as many different data situations as possible, we use four data sources that together comprise 2,403 fertility schedules.

Human Fertility Database/Human Mortality Database

We first benchmark the estimators against the HFD (n.d.), the most complete and accurate data set available on current and historical patterns of human fertility. The HFD covers fertility schedules for 31 countries between 1891 and 2015, containing 1,958 country-years of age-specific and total fertility rates. These are listed in Table A1 in the online appendix.

For each country-year in the HFD, we link the corresponding population data (i.e., the age pyramid) and the q_5 value from the HMD (n.d.). When joined, the HFD/HMD data include true target values for TFR and input data (C, W_{15}, …, W_{45}, q_5) for the five estimators.

[4] A Poisson model assumes equality between the mean and variance of the number of surviving children. This strong assumption generally does not hold in practice (e.g., Barakat 2017: figure 1). Individual heterogeneity in age-specific rates would tend to produce overdispersion (variance > mean), whereas strong social norms about childbearing might tend to produce underdispersion (variance < mean). In a comprehensive empirical study of cohort parity, Barakat (2014) found evidence for effects in both directions. Underdispersion is more common at low parities and vice versa. The good performance of the *bTFR* estimator in our empirical tests suggests that the Poisson model is adequate for estimating *TFR* from age-sex distributions.

Demographic and Health Surveys

HFD/HMD data are highly accurate but cover a fairly narrow range of demographic conditions. HFD populations are mainly in contemporary developed countries with relatively low fertility and mortality rates.

To evaluate the estimators under a broader set of conditions, we also test against Demographic and Health Survey (DHS) data. DHS data include nationally representative household surveys for monitoring population health in 47 countries all with sample TFR estimates. For 118 country-periods, we use the DHS API (Demographic and Health Surveys (DHS) Program 2019) to download estimated TFR, number of women aged 15–49, number of children under age 5, and q_5. We use IPUMS-DHS (Boyle et al. 2017) to download the corresponding numbers of women by five-year age group. The combined DHS data include a (noisy but unbiased) estimate of the target value for *TFR*, and the input data (C, W_{15}, …, W_{45}, q_5) for the five estimators.

U.S. County Fertility

Combining HFD/HMD and DHS data allows us to evaluate our methods at the national level. To evaluate the estimators at subnational geographies, we use age-sex distributions from the 2010 decennial census to produce *xTFR* and *iTFR* estimates for every county in the United States. We evaluate the accuracy of these estimates by comparing to published county-level TFR values from the National Center for Health Statistics (NCHS), obtained via the Centers for Disease Control (CDC) Wide Ranging Online Data for Epidemiological Research (WONDER) tool.

The NCHS publishes highly accurate subnational fertility information in the United States. However, for privacy reasons, the NCHS does not publish fertility information for U.S. counties with populations less than 100,000. As a result, we can compare estimates to true county-level TFR values for only 524 of the approximately 3,000 U.S. counties.

Nonhuman Data

The basic *iTFR* variant requires information only on a population's age-sex structure. Population pyramids are not limited to humans, so *iTFR* could in principle be used to estimate total fertility in nonhuman populations if age-sex distributions were accurate. To test this proposition, we assemble age-specific fertility and population data for 11 nonhuman species (eight wild and one captive primate species, one wild lion species, and one wild seal species), reported in Table 2.

These populations vary substantially, allowing us to assess whether the method works across species with very different levels and age patterns of fertility. In contrast to humans, for whom scientists typically demarcate menarche and menopause at ages 15 and 50 years, respectively, menarche among the 11 species ranges from a low of age 2 for sifakas (*P. verreauxi*) and African lions (*P. leo*) to a high of 11 years for chimpanzees (*P. troglodytes*). Reproductive age spans range from a low of 7 years for Thomas's langurs (*P. thomasi*) to a high of 38 years for chimpanzees. These species display reproductive age spans, fertility schedules, and TFRs that differ greatly from those of humans.

Table 2 Nonhuman fertility data

Species and Source	Location	α	β	${}_1P_0$	${}_{\beta-\alpha}W_{\alpha}$	TFR
Sifaka (*P. verreauxi*)[a]	Madagascar	2	31	708	2,073	10.67
African Lion (*P. leo*)[b]	Tanzania	2	17	2,643	3,819	10.38
Capuchin (*C. capucinus*)[a]	Costa Rica	5	24	189	423	9.82
Baboon (*P. cynocephalus*)[a]	Kenya	4	23	1,098	2,465	9.37
Muriqui (*B. hypoxanthus*)[a]	Brazil	7	40	376	1,347	8.89
Blue Monkey (*C. mitis*)[a]	Kenya	4	30	486	1,542	8.69
Gorilla (*G. beringei*)[a]	Rwanda	8	40	258	1,049	8.00
Macaque (*M. nemestrina*)[c]	Captive	3	22	2,368	7,494	6.91
Chimpanzee (*P. troglodytes*)[a]	Tanzania	11	49	189	1,195	6.29
Northern Fur Seal (*C. ursinus*)[d]	—	3	19	2,096	6,436	6.10
Thomas's Langur (*P. thomasi*)[e]	Indonesia	4	11	161	305	3.67

Notes: α and β are the first and last ages with observed nonzero fertility rates for each species. ${}_1P_0$ is the number of individuals younger than 1 year old. ${}_{\beta-\alpha}W_{\alpha}$ is the number of females of reproductive age. TFR is observed total fertility.

[a] Source is Bronikowski et al. (2016a, b).

[b] Source is Packer et al. (1998).

[c] Source is Ha et al. (2000).

[d] Source is Barlow & Boveng (1991).

[e] Source is Wich et al. (2007).

Demographic data for nonhuman populations are collected very differently from human data. Living individuals must be directly observed, their ages must be estimated, and their sex may or may not be known. Despite these differences, it is interesting to evaluate the effectiveness of estimating lifetime fertility from age structure for other species.

Evaluation

Overall Error

We begin by investigating TFR estimation errors over all available test cases for human data. Figure 1 reports the 10th, 50th, and 90th percentiles of the absolute error ($|est - obs|$) for all methods in the HMD/HFD, DHS, and U.S. county data sets.

All methods produce quite accurate results using all three data sources for almost all the populations under study. Only the *xTFR* variant for DHS data produces estimates with the median absolute error above 0.25 births/woman. Median absolute errors are less than 0.10 births/woman in most data sets.

In general, more sophisticated estimators have lower average errors. Ordering by median errors shows that the simplest estimator, *iTFR*, has the poorest (although still very good) performance; that adding age structure detail and/or mortality corrections

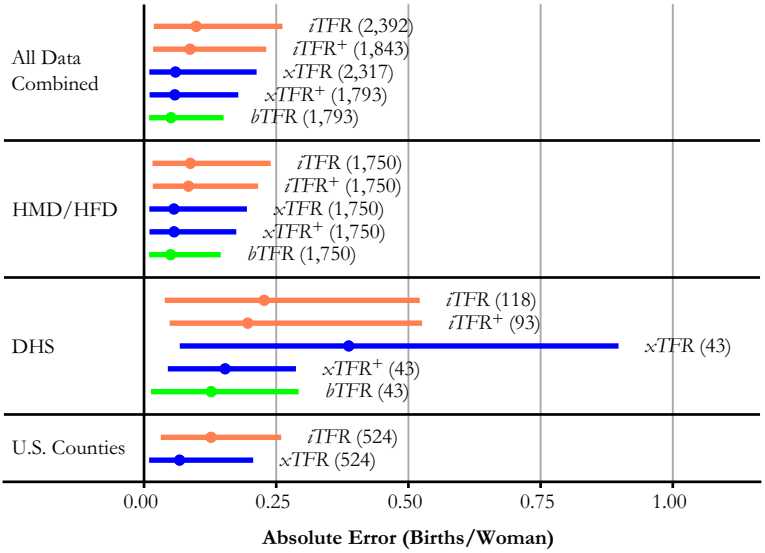

Fig. 1 Absolute error (births/woman) in TFR over alternative methods and data sets. Solid dots are at median error for each method and data set. Horizontal bars extend from the 10th to 90th percentile of error. Numbers in parentheses indicate the count of schedules for which it is possible to use each method.

(*xTFR*, *iTFR*+, and *xTFR*+) reduces errors further; and that the most complex model (*bTFR*) has the smallest average errors.

There is one important exception to the general "fancier is better" rule. In populations with high mortality and fertility rates—exemplified in our data by DHS countries—adding details about the age distribution of reproductive-age women while ignoring child mortality (i.e., changing *iTFR* → *xTFR*) actually makes estimates worse. Why? Recall from Eq. (4) that the true $C / W \rightarrow TFR$ multiplier has two parts: $1/s$ for child mortality correction, and $1/p$ for age structure correction. *iTFR* assumes $1/s = 1$ and $1/p = 7$. In a high-mortality, high-fertility population, the true values of the two components actually tend to be greater than 1 (more than one birth per living child) and less than 7 (children born recently represent less than one-seventh of the population's lifetime births because there are relatively few old women). In such situations, *iTFR* underestimates one component of the multiplier ($1/s$) and overestimates the other ($1/p$), while *xTFR* underestimates ($1/s$) and gets ($1/p$) about right. Compensating errors for *iTFR* mean that it actually performs better than the more sophisticated *xTFR* approach in a high-mortality, high-fertility setting.

This leads to one important caveat. If mortality estimates are unavailable, then *iTFR* is preferable to *xTFR* in a population with suspected high mortality.

Errors for Nonhuman Species

To test the generalizability of the method, we examine the accuracy of the *iTFR* estimator in 11 nonhuman populations described in Table 2. We find that *iTFR* accurately estimates total fertility among these species (Fig. 2). These results suggest that the method captures fundamental properties governing mammalian fertility and that it could be valuable in other studies with nonhuman populations.

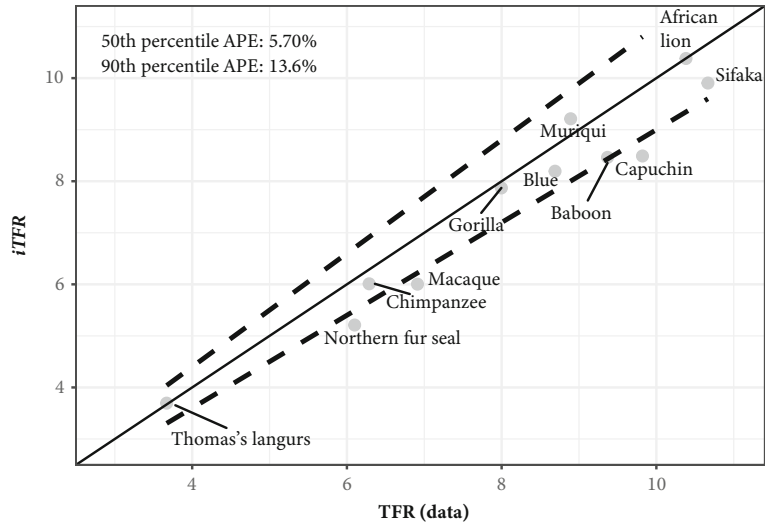

Fig. 2 Fertility estimates for animal populations. *iTFR* estimates from nonhuman age-sex distributions. Observed TFR versus *iTFR* estimates for the species listed in Table 2. Estimates match observations along the 45-degree line; dashed lines represent ±10% errors.

Sensitivity to TFR Level, Population Size, and Period

Figure 3 reports the accuracy of *iTFR*, *xTFR*, and *bTFR* estimators for the HFD/HMD and DHS data combined for different TFR levels, population sizes, and historical periods. Table 3 reports summary measures of the accuracy for all five estimators using the same combined HFD/HMD and DHS data as well as U.S. counties. Overall, we find good agreement between estimated and observed TFRs for all five estimators (Fig. 3, panels a, b, and c; and Table 3).

Demographic estimators are typically more accurate for larger populations (because of the law of large numbers) and for more recent periods (because of improved data collection practices). However, we find that error rates are independent of population size (Fig. 3, panels d, e, and f) and are fairly stable across time (Fig. 3, panels g, h, and i), suggesting scale and temporal independence uncommon in other indirect methods.

Even the simplest and least accurate of the five variants, *iTFR*, predicts the total fertility rate with absolute errors of less than 0.09 births/woman in one-half of the HFD and DHS populations and less than 0.26 births/woman in 90% of the populations (Table 3). Absolute percentage errors for *iTFR* are also quite small relative to most indirect demographic estimators: 50% of errors are within 4.6% of the true TFR, and 90% are within 10.8%. As shown in Fig. 3 and Table 3, the additional information contained in the *xTFR* and *bTFR* estimators produce even smaller errors. In short, we find that for national populations in countries with accurate data and (mostly) low mortality, accurate TFR estimates from population pyramids are possible.

Errors in Subnational Estimates

It is possible that coefficients derived at the national level could prove ineffective in estimating fertility at the subnational level (e.g., Tuchfeld et al. 1974). Table 3 reports

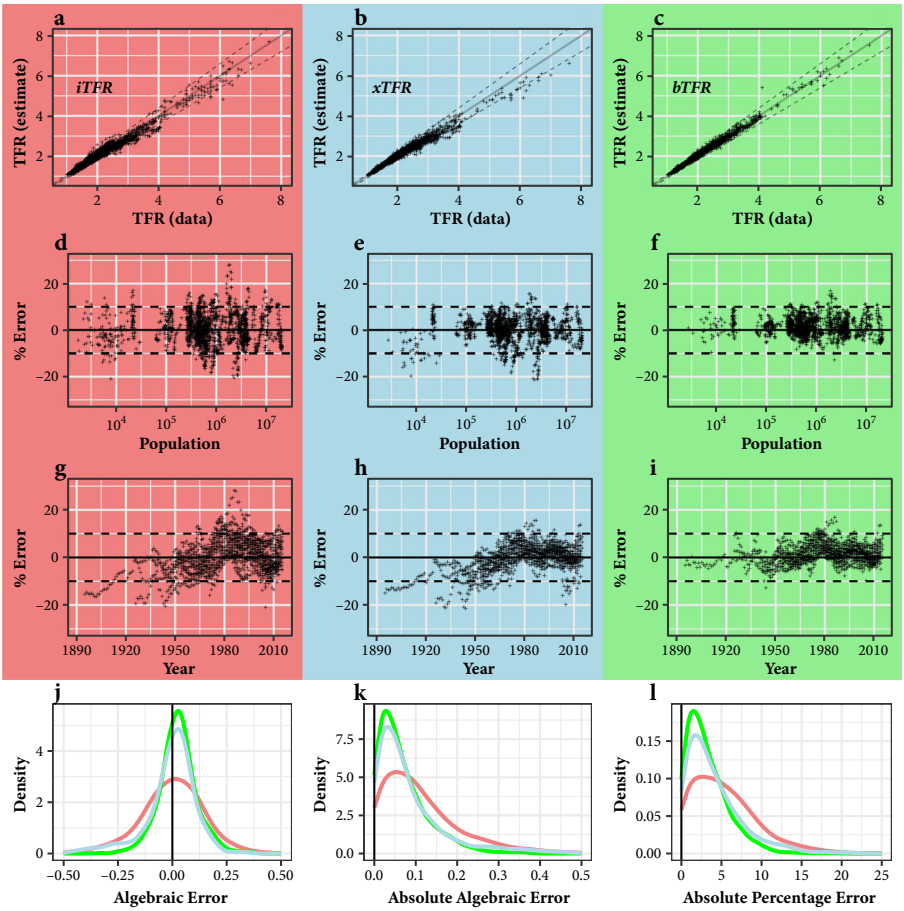

Fig. 3 Estimated TFR from population pyramids. Performance of three variants in HFD and DHS data. Panels a, d, and g use *iTFR*; panels b, e, and h use *xTFR*; panels c, f, and i use *bTFR*; and panels a, b, and c plot estimated TFR against the observed five-year average TFR. The solid line is $Y = X$, and the dashed lines are ±10%. Panels d, e, and f illustrate the percentage error against population size. The dashed lines represent errors of ±10%. Panels g, h, and i plot percentage errors against the year in which the population pyramid is observed. Panel j plots the distribution of algebraic errors for each method (*est* – *obs*). Panel k plots the distribution of absolute algebraic errors. Panel l plots the distribution of absolute percentage errors. For all variants, estimates are accurate over many scales and times.

the errors associated with both the *iTFR* and *xTFR* methods for U.S. counties that also have corresponding observed total fertility rates. These errors are on par with the errors observed using the HMD/HFD data, demonstrating important consistency in low error rates across a variety of scales.

Sensitivity to Child Mortality

Our derivations for the *iTFR* and *xTFR* assume that child mortality is negligible, and those estimators are likely to underestimate fertility when it is not. We show this relationship in Fig. 4 using data from the HMD/HFD and DHS, where *iTFR* and

Table 3 Summary statistics for the five variants using data from the HMD/HFD and DHS and U.S. counties

Data	Method Family	*n*	50th Percentile Absolute Error	90th Percentile Absolute Error	50th Percentile APE[a]	90th Percentile APE[a]
DHS	*iTFR*	118	0.23	0.52	4.7	10.5
	iTFR$^+$	93	0.20	0.53	4.0	11.1
	xTFR	43	0.39	0.90	8.4	14.0
	xTFR$^+$	43	0.15	0.29	2.7	6.6
	bTFR	43	0.13	0.29	2.3	5.3
HMD/HFD	*iTFR*	1,750	0.09	0.24	4.6	10.7
	iTFR$^+$	1,750	0.08	0.22	4.4	10.3
	xTFR	1,750	0.06	0.19	3.0	8.2
	xTFR$^+$	1,750	0.06	0.17	2.9	7.4
	bTFR	1,750	0.05	0.15	2.6	6.6
U.S. Counties	*iTFR*	524	0.13	0.26	6.5	12.8
	xTFR	524	0.07	0.21	3.3	10.1

[a] APE = absolute percentage error.

xTFR produce increasing errors as child mortality increases. Notice that the *iTFR*$^+$, *xTFR*$^+$, and *bTFR* variants largely correct for higher mortality levels. Thus, in countries or periods with high infant and child mortality, the *iTFR*$^+$, *xTFR*$^+$, and *bTFR* variants are more appropriate.

Extensions

Accurate estimation of TFR from age-sex pyramids greatly expands our ability to estimate fertility across varying geographies, periods, and subpopulations. To demonstrate the flexibility of the method, we produce TFR estimates for three cases in which direct TFR estimation is impossible.

Subnational Fertility in Africa

We use data from WorldPop's gridded population age-structure data for the year 2015 (Tatem et al. 2013) in conjunction with q_5 estimates from the United Nations World Population Prospects 2017 (United Nations 2017) to produce subnational estimates of *iTFR*$^+$ for Africa. Scholars have increasingly published subnational estimates of demographic indicators to monitor progress toward the United Nations Sustainable Development Goals (SDGs) (Golding et al. 2017; Graetz et al. 2018; Osgood-Zimmerman et al. 2018), and our framework allows a nearly unprecedented level of geographic detail regarding fertility (Fig. 5).

Historical Fertility in Europe

We also extend our analysis of the HMD by producing fertility estimates for all 2,955 country-years of data in the HMD (an additional 1,000 country-years' of estimates prior to

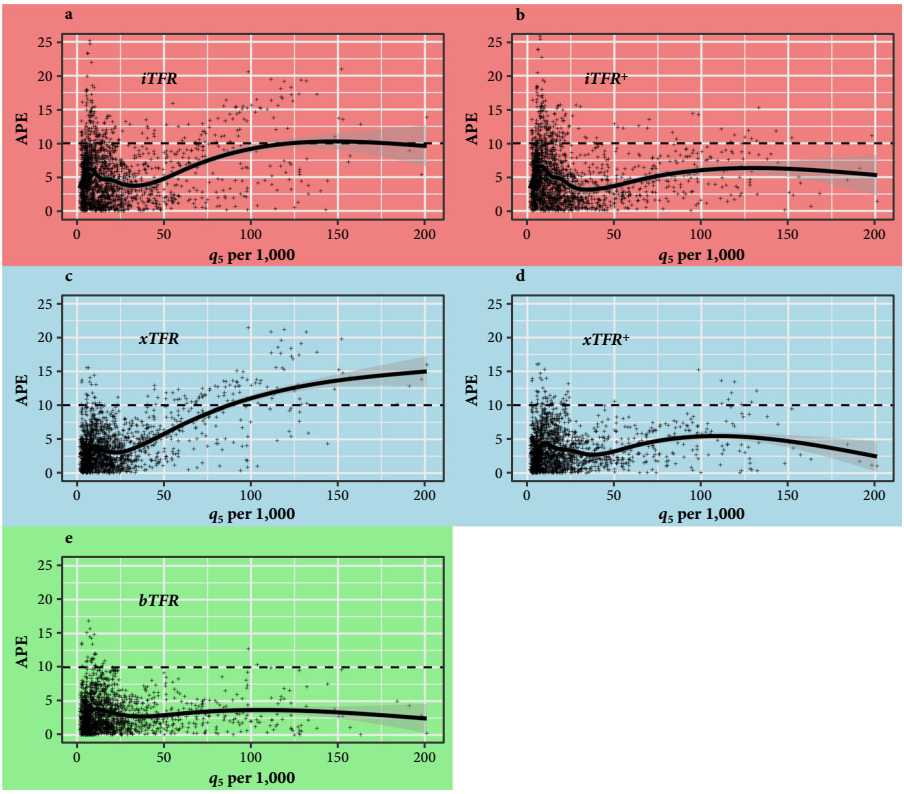

Fig. 4 Absolute percentage errors (APE) against q_5 values in the HMD and DHS. We compare the performance of the five variants against observed q_5 mortality rates. As q_5 values increase, the APE also increases in the *iTFR* and *xTFR* variants. This is corrected in the *iTFR*+, *xTFR*+, and *bTFR* variants, which incorporate estimated child mortality.

the collection of detailed birth records). From this large historic volume of data, we highlight our findings in four example countries: France, Italy, the Netherlands, and Sweden (Fig. 6). Sweden began tabulating the detailed birth records necessary for TFR calculation in 1891; France, in 1946; the Netherlands, in 1950; and Italy, in 1954. However, these countries collected both mortality and age-sex data considerably earlier (1751 for Sweden, 1816 for France, 1850 for the Netherlands, and 1872 for Italy). By using the *bTFR* method, we can reconstruct historical TFRs to create a time series of fertility data well before age-specific birth collection began, significantly expanding our ability to explore historical fertility patterns from up to 250 years ago.

Fertility by Income and Race in the United States

The complex connections between fertility and household income have always interested demographers (Becker 1960; Jones et al. 2008). However, analysis is limited because birth certificates do not include economic information, and very few surveys include both income and fertility questions. Estimation of fertility levels from population composition can expand our ability to learn about fertility-income correlations in different social groups.

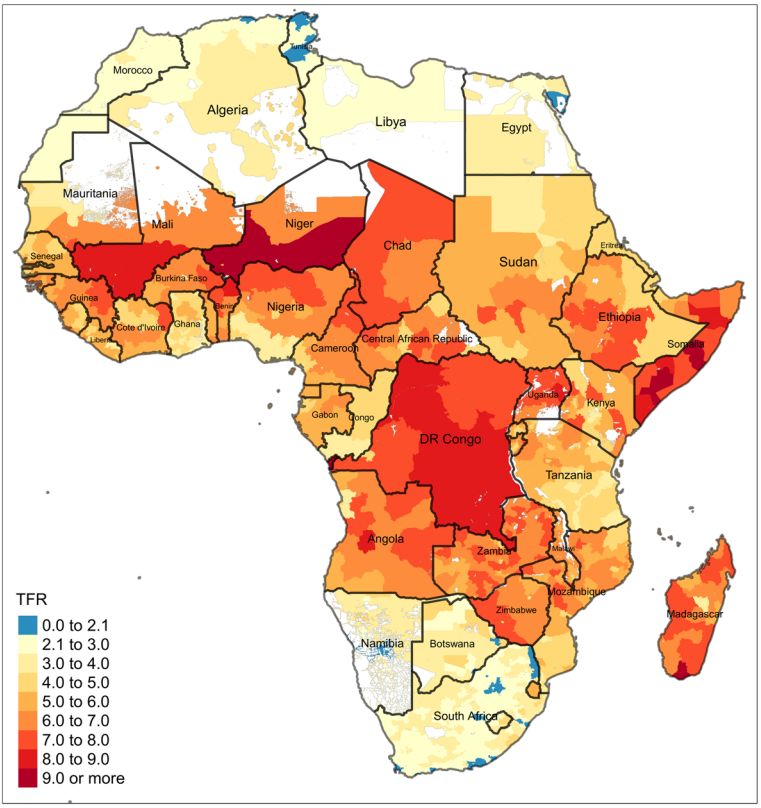

Fig. 5 Estimating subnational fertility rates. We use the *iTFR*+ method to estimate subnational total fertility rates for the African continent for 2010–2015 using data from WorldPop and the United Nations WPP 2017.

Figure 7 provides an example. We use the *xTFR* method to estimate TFRs conditional on both race (white/non-White) and household income level in the United States, using data on the age-sex composition of households in different income strata from the Current Population Survey (CPS). Data for this figure come from aggregated 2010–2018 March Economic Supplements, downloaded from IPUMS (Flood et al. 2018). Indirect methods based on age-sex data allow us to produce estimates of TFR by income groups and to further disaggregate by race. Among both Whites and non-Whites, there is a definite U-shaped relationship, with the highest fertility levels in the poorest and richest American households.

Here we provide these examples only as a proof of concept: indirect fertility estimation identifies intriguing relationships that would not be estimable by other means, which clearly merits further study.

Conclusion

We examined our framework's errors using high-quality age pyramids and fertility data. With a few minor caveats, we conclude that indirect estimators yield accurate TFR estimates when age-sex input data is accurate.

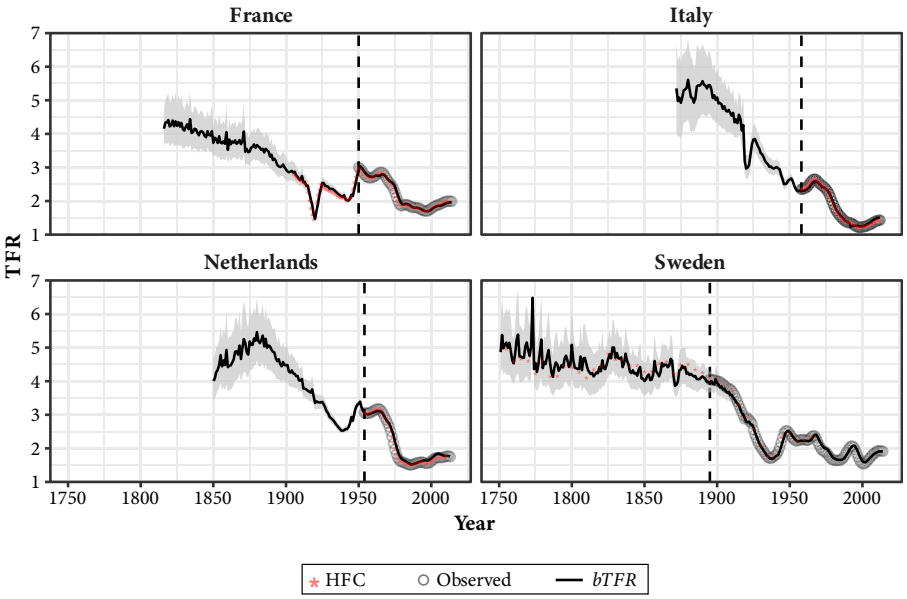

Fig. 6 Estimating historical fertility. *bTFR* estimates of period fertility rates in four European countries using HMD historical age-sex and child mortality data. Shaded regions represent 90% posterior probability intervals; open circles are observed TFRs from the HFD; vertical dashed lines refer to the earliest data in the HFD. Red stars are average TFRs over the preceding five-year period for the earliest series with a vital records source from the Human Fertility Collection (HFC n.d.).

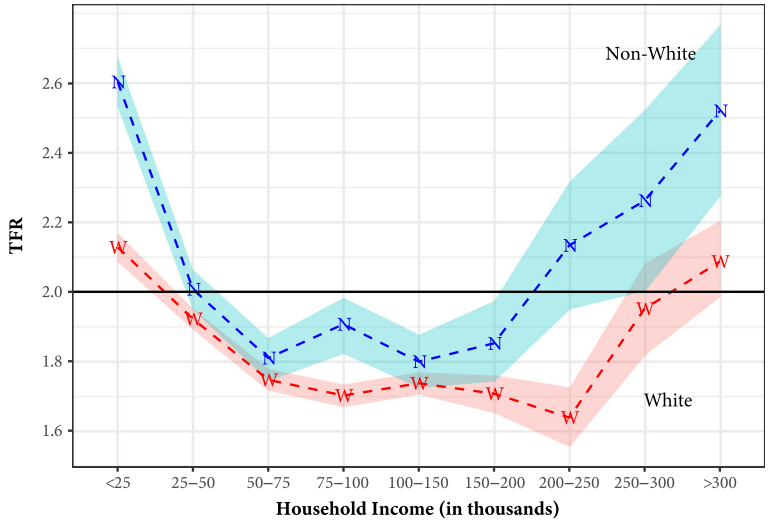

Fig. 7 Total fertility rate (*xTFR*) by race and household income level. We estimate TFR from age-sex distributions within race-income categories using the U.S. Current Population Survey (CPS) March Social and Economic Supplements, combined over 2010–2018. White corresponds to those reporting their race as White only. Non-White corresponds to all other survey respondents. Shaded regions represent confidence intervals (5% to 95%) estimated from 1,000 bootstrap samples in which households in each race-income category are drawn randomly with replacement from the set of all CPS households.

Researchers should use caution, however, when applying our framework in data environments with potentially deficient inputs. Our methods produce good estimates of *TFR*, but they require accurate age-sex counts. Underenumeration of children aged 0–4 is a well-known problem with census data (Ewbank 1981; O'Hare 2014, 2015), and misreporting of children aged 0–4 will yield inaccurate estimates of total fertility in our framework. Future extensions could adjust for underenumeration, either by adding an undercount multiplier to Eq. (4) or by including a prior distribution for undercount in the *bTFR* model.

Demographers should use expert judgement when choosing which variant to employ. For instance, in populations with known or suspected high child mortality, one should likely estimate TFR using $iTFR^{+}$, $xTFR^{+}$, or *bTFR* to correct for child mortality (if q_5 estimates are available). In choosing the three example extensions in the earlier Extensions section, we chose the variant to fit both the data available and known demographic characteristics of the population. We know that Africa tends to have high child mortality, but we are also cautious about the accuracy of WorldPop's age-structure data. This led us to $iTFR^{+}$, which corrects for child mortality but does not use the detailed age distribution for women of childbearing ages. Similarly, the HMD contains high-quality data, but the further back in time one goes, the more important uncertainty about child mortality becomes. In this situation, *bTFR* is the appropriate method. To estimate U.S. fertility conditional on household income and race, we do not have child mortality available for these populations. However, U.S. child mortality is quite low, and the age structure among reproductive-age women is quite variable for small subpopulations. These considerations make *xTFR* the most appropriate estimator. Scholars should use similar judgements when using our framework to answer their own research questions.

Our framework's flexible data requirements allow researchers to select the variant that conforms to the available data while offering high confidence for estimates. As we show in our example extensions, this approach opens the door to fertility analyses for many populations of interest to sociologists (Lesthaeghe 2014), economists (Hotz et al. 1997), anthropologists (Greenhalgh 1995), epidemiologists (Paulson et al. 2002), historians (Woods 2000), and population geographers (Sorichetta et al. 2015).

There is now increased demand for high-resolution gridded population data sets for climate change research and SDGs (Cincotta et al. 2000; Jones et al. 2015; Golding et al. 2017). Because our methods work well for small populations, scientists could use them to estimate small-area fertility levels and changes as inputs to gridded population projections or for gridded fertility-level data sets.

Because they rely on basic, commonly collected census data, the parameter-free, scale-, time-, and species-robust techniques can estimate total fertility even in areas without detailed demographic data. We anticipate this estimation framework will open new lines of inquiry into human fertility patterns.

Replication Files

(https://github.com/mathewhauer/iTFR-replication). The analyses were performed in *R* (R Core Team 2018). For the *bTFR* variant, we used the *rstan* package (Stan Development Team 2016) to interface with Stan (Carpenter et al. 2017).

Acknowledgments We thank A. Bronikowski, R. Lawler, and S. Alberts for their assistance with their primate data, and B. Jarosz and K. Devivo for feedback on earlier versions.

References

Abel, G. J., Barakat, B., Samir, K. C., & Lutz, W. (2016). Meeting the sustainable development goals leads to lower world population growth. *Proceedings of the National Academy of Sciences, 113,* 14294–14299.

Barakat, B. (2014). *Revisiting the history of fertility concentration and its measurement* (VID Working Paper 1/2014). Vienna, Austria: Vienna Institute of Demography. Retrieved from https://www.econstor.eu/bitstream/10419/97017/1/784170290.pdf

Barakat, B. (2017). Generalised count distributions for modelling parity. *Demographic Research, 36,* 745–758. https://doi.org/10.4054/DemRes.2017.36.26

Barlow, J., & Boveng, P. (1991). Modeling age-specific mortality for marine mammal populations. *Marine Mammal Science, 7,* 50–65.

Becker, G. S. (1960). An economic analysis of fertility. In Universities-National Bureau Committee for Economic Research (Ed.), *Demographic and economic change in developed countries* (pp. 209–240). New York, NY: Columbia University Press.

Bogue, D., & Palmore, J. (1964). Some empirical and analytic relations among demographic fertility measures, with regression models for fertility estimation. *Demography, 1,* 316–338.

Boyle, H. E., King, M., & Matthew, S. (2017). *IPUMS-Demographic and Health Surveys: Version 4.1* [Dataset]. Retrieved from 10.18128/D080.V4.1

Bronikowski, A. M., Cords, M., Alberts, S. C., Altmann, J., Brockman, D. K., Fedigan, L. M., … Morris, W. F. (2016a). *Data from: Female and male life tables for seven wild primate species* [Dryad dataset]. Retrieved from https://doi.org/10.5061/dryad.v28t5

Bronikowski, A. M., Cords, M., Alberts, S. C., Altmann, J., Brockman, D. K., Fedigan, L. M., … Morris, W. F. (2016b). *Female and male life tables for seven wild primate species* [Dryad dataset]. Retrieved from https://doi.org/10.5061/dryad.v28t5

Carpenter, B., Gelman, A., Hoffman, M., Lee, D., Goodrich, B., Betancourt, M., … Riddell, A. (2017). Stan: A probabilistic programming language. *Journal of Statistical Software, 76*(1), 1–32. https://doi.org/10.18637/jss.v076.i01

Cincotta, R. P., Wisnewski, J., & Engelman, R. (2000). Human population in the biodiversity hotspots. *Nature, 404,* 990–992. https://doi.org/10.1038/35010105

Demographic and Health Surveys Program (DHS). (2019). *The DHS Program indicator data API.* Available from api.dhsprogram.com

Ewbank, D. C. (1981). *Age misreporting and age-selective underenumeration: Sources patterns and consequences for demographic analysis*. Washington, DC: National Academies Press.

Flood, S., King, M., Rodgers, R., Ruggles, S., & Warren, J. R. (2018). *IPUMS-Current Population Survey: Version 6.0* [Dataset]. Retrieved from https://doi.org/10.18128/D030.V6.0

Gerland, P., Raftery, A. E., Sevčíková, H., Li, N., Gu, D., Spoorenberg, T., … Lalic, N. (2014). World population stabilization unlikely this century. *Science, 346,* 234–237.

Golding, N., Burstein, R., Longbottom, J., Browne, A. J., Fullman, N., Osgood-Zimmerman, A., … Hay, S. I. (2017). Mapping under-5 and neonatal mortality in Africa, 2000–15: A baseline analysis for the Sustainable Development Goals. *Lancet, 390,* 2171–2182.

Graetz, N., Friedman, J., Osgood-Zimmerman, A., Burstein, R., Biehl, M. H., Shields, C., … Hay, S. I. (2018). Mapping local variation in educational attainment across Africa. *Nature, 555,* 48–53.

Greenhalgh, S. (1995). *Situating fertility: Anthropology and demographic inquiry*. Cambridge, UK: Cambridge University Press.

Ha, J. C., Robinette, R. L., & Sackett, G. P. (2000). Demographic analysis of the Washington Regional Primate Research Center pigtailed macaque colony, 1967–1996. *American Journal of Primatology, 52,* 187–198.

Hauer, M., Baker, J., & Brown, W. (2013). Indirect estimates of total fertility rate using child woman/ratio: A comparison with the Bogue-Palmore method. *PLoS One, 8*(6), e67226. https://doi.org/10.1371/journal.pone.0067226

Hotz, V. J., Klerman, J. A., & Willis, R. J. (1997). The economics of fertility in developed countries. In M. R. Rosenzweig & O. Stark (Eds.), *Handbook of population and family economics* (Vol. 1A, pp. 275–347). Amsterdam, the Netherlands: Elsevier.

Human Fertility Collection. (n.d.). Rostock, Germany: Max Planck Institute for Demographic Research, and Vienna, Austria: Vienna Institute of Demography. Available from www.fertilitydata.org

Human Fertility Database. (n.d.). Rostock, Germany: Max Planck Institute for Demographic Research, and Vienna, Austria: Vienna Institute of Demography. Available from www.humanfertility.org

Human Mortality Database. (n.d.). Berkeley: University of California, Berkeley, and Rostock, Germany: Max Planck Institute for Demographic Research. Available from www.mortality.org

Jones, B., O'Neill, B. C., McDaniel, L., McGinnis, S., Mearns, L. O., & Tebaldi, C. (2015). Future population exposure to US heat extremes. *Nature Climate Change, 5,* 652–655.

Jones, L. E., Schoonbroodt, A., & Tertilt, M. (2008). *Fertility theories: Can they explain the negative fertility-income relationship?* (NBER Working Paper No. 14266). Cambridge, MA: National Bureau of Economic Research.

Lesthaeghe, R. (2014). The second demographic transition: A concise overview of its development. *Proceedings of the National Academy of Sciences, 111,* 18112–18115.

O'Hare, W. P. (2014). *Historical examination of net coverage error for children in the U.S. decennial census: 1950 to 2010* (Survey Methodology Report #2014-03). Washington, DC: Center for Survey Measurement Study Series, U.S. Census Bureau.

O'Hare, W. P. (2015). Coverage of young children in the census: An international comparative perspective. In *The undercount of young children in the U.S. decennial census* (pp. 73–82). Cham, Switzerland: Springer.

Osgood-Zimmerman, A., Millear, A. I., Stubbs, R. W., Shields, C., Pickering, B. V., Earl, L., … Hay, S. I. (2018). Mapping child growth failure in Africa between 2000 and 2015. *Nature, 555,* 41–47.

Packer, C., Tatar, M., & Collins, A. (1998). Reproductive cessation in female mammals. *Nature, 392,* 807–811.

Paulson, R. J., Boostanfar, R., Saadat, P., Mor, E., Tourgeman, D. E., Slater, C. C., … Jain, J. K. (2002). Pregnancy in the sixth decade of life: Obstetric outcomes in women of advanced reproductive age. *JAMA, 288,* 2320–2323.

R Core Team. (2016). R: A Language and Environment for Statistical Computing [Software]. Vienna, Austria: R Foundation for Statistical Computing. Available from https://www.R-project.org/

R Core Team. (2018). R: A Language and Environment for Statistical Computing [Software]. Vienna, Austria: R Foundation for Statistical Computing. Available from https://www.R-project.org/

Rele, J. (1967). Fertility analysis through extension of stable population concepts. Berkeley: Institute of International Studies, University of California. Retrieved from https://books.google.com/books?id=K3cwAAAAMAAJ

Schmertmann, C. P., & Hauer, M. E. (2019). Bayesian estimation of total fertility from a population's age–sex structure. *Statistical Modelling, 19,* 225–247.

Sorichetta, A., Hornby, G. M., Stevens, F. R., Gaughan, A. E., Linard, C., & Tatem, A. J. (2015). High-resolution gridded population datasets for Latin America and the Caribbean in 2010, 2015, and 2020. *Scientific Data, 2,* 150045. https://doi.org/10.1038/sdata.2015.45

Stan Development Team. (2016). RStan: The R Interface to Stan [R package version 2.14.1]. Retrieved from http://mc-stan.org/

Tatem, A. J., Garcia, A. J., Snow, R. W., Noor, A. M., Gaughan, A. E., Gilbert, M., & Linard, C. (2013). Millennium development health metrics: Where do Africa's children and women of childbearing age live? *Population Health Metrics, 11,* 11. https://doi.org/10.1186/1478-7954-11-11

Tuchfeld, B. S., Guess, L. L., & Hastings, D. W. (1974). The Bogue-Palmore technique for estimating direct fertility measures from indirect indicators as applied to Tennessee counties, 1960 and 1970. *Demography, 11,* 195–205.

United Nations. (2017). *World population prospects—2017 revision: Methodology of the United Nations population estimates and projections* (Report). New York, NY: United Nations.

U.S. Census Bureau. (2016). *U.S. Census Bureau international* [Data set]. Available from https://www.census.gov/data-tools/demo/idb/informationGateway.php

Wachter, K. W. (2014). *Essential demographic methods*. Cambridge, MA: Harvard University Press. Retrieved from https://books.google.com/books?id=hAWMAwAAQBAJ

Wich, S. A., Steenbeek, R., Sterck, E. H., Korstjens, A. H., Willems, E. P., & Van Schaik, C. P. (2007). Demography and life history of Thomas langurs *(Presbytis thomasi). American Journal of Primatology, 69,* 641–651.

Wilmoth, J., Zureick, S., Canudas-Romo, V., Inoue, M., & Sawyer, C. (2012). A flexible two-dimensional mortality model for use in indirect estimation. *Population Studies, 66,* 1–28.

Woods, R. (2000). *The demography of Victorian England and Wales* (Vol. 35). Cambridge, UK: Cambridge University Press.